Creating selective directional interactions with defects caused by subnanometre-ordered ligand domains on the surface of colloidal metal nanoparticles for the purpose of directed self-assembly.

by

Brian Neltner

Submitted to the Department of Materials Science and Engineering
in partial fulfillment of the requirements for the degree of

Bachelor of Science in Materials Science and Engineering

at the

MASSACHUSETTS INSTITUTE OF TECHNOLOGY

May 2005 [June 2005]

Author .....
Department of Materials Science and Engineering
May 20, 2005

Certified by .....
Professor Francesco Stellacci
Finmeccanica Assistant Professor of Materials Science and Engineering
Thesis Supervisor

Accepted by .....
Professor Donald R. Sadoway
John F. Elliott Professor of Materials Chemistry
Chairman, Committee for Undergraduate Studies

Acknowledgments

With many thanks to the Department of Materials Science and Engineering, as well as the Microscopy Facilities for advice and support. Also many thanks to the Sunmag research group, specifically Professor Francesco Stellacci and Markus Brunnbauer for technical advice, and Ben Wunsch for his many hours spent doing T.E.M. on the final samples.

Contents

List of Figures

Chapter 1

Introduction

The ability to utilize directional, specific bonds are a fundamental property of atoms which has allowed us to predictably create molecules of consistent geometry and composition for centuries. One fundamental difference between a true atom and a nanoparticle is that to date, nanoparticles do not possess this property.

Chapter two describes the experimental plan chosen for giving the nanoparticles specific directional binding ability, as well as the motivations for the chosen parameters. Specifically, it includes information on the attempts made to use peptide bonds to create long chains of nanoparticles.

Chapter three describes the alteration to the experiment discussed in chapter two in order to allow for using DNA to create linear chains.

Chapter four describes the design of the chain data analysis software, as well as what the extracted data demonstrated about the nanoparticle chains.

Chapter five discusses the conclusions of the chain linking and analysis software, and suggests future experiments and improvements which could be made to make the data more compelling.

Chapter six discusses the attempts to date for creating more complicated shapes as well as directions for future research.

1.1 Motivation for the creation of selective, directional bonds.

A huge advantage of using nanoparticles to build devices is that it is easy to do coupling chemistry- the strong interaction of a thiol with gold allows for surface modification through a self-assembled monolayer (SAM) on the surface to virtually any chemistry desired through an alkane thiol. Unfortunately, the inability to create directional bonds with nanoparticles is a huge limiting factor in the use of self-assembly to create devices with these materials.

The ability to create a consistent directional bond would allow for the design of anything from linear chains for use in photonics to vast self-assembled superstructures in two or three dimensions. By producing nanoparticles with these bonds, we open up a vast new field of super-molecular chemistry.

1.2 Background

A nanoparticle is a "zero-dimensional" system where electrons in a periodic potential are subject to a constraint in position space.

In a periodic potential, the result of solving for the allowed electron energies is a band structure. In this band structure, electron states have energy spacings roughly equal to the width of the band divided by the number of lattice constants from one side of the nanoparticle to the other. For a bulk material, this means that the spacing between electron states is effectively zero (the number of lattice constants from one side to the other is infinite). However, the size confinement of a nanoparticle results in a finite energy spacing (dependent on material type, shape, and diameter). This energy spacing can become large enough to prevent electrons at a given thermal energy from being promoted between energy levels even within what would have otherwise been an allowed energy band, which leads to a variety of interesting effects, such as single electron transistor behaviour.[2]

The discrete nature of the electron states in a nanoparticle also produce interesting optical properties; quantum dots, a type of semiconducting nanoparticle, shows a size dependant flourescence spectra. By putting specific binding agents on the surface of the quantum dot which are sensitive to a biological agent, simple flourescence can be used to determine whether or not the agent is present in a sample.[3]

The next most important aspect about nanoparticle behaviour is their intrinsically high surface area to volume ratio. A typical collection of nanoparticles might well have 100 m^2 of surface area per gram. This high surface area means that they have an extremely high reactivity compared to the bulk phase (the ratio of so-called "dangling bonds", or unsatisfied potential bonds, to total bonds is very high), and that surface energy plays an extremely important role in determining their behaviour.

This allows one to dissolve gold crystals where it would ordinarily only be possible to get gold in a liquid form at high temperatures. A thiol molecule will bind very strongly to gold, resulting in a SAM on the surface of a gold nanoparticle protecting it from combining with other particles.[4] By using a thiol activated at the other end with a molecule readily dissolved in the desired solvent, it is possible to make it energetically favourable for the entire cluster to enter a solution despite the density mismatch of the gold cluster to the solvent.

For example, by using mercaptohexanol, a hexane molecule with a thiol group at one end and an alcohol group on the other, it is possible to create a SAM on the surface of the gold particles which then displays only alcohol groups. This particle is then readily soluble in water. This property also allows for the potential of using nanoparticles to increase the solubility of ordinarily poorly water soluble drugs.[5]

The ability to dissolve nanoparticles of crystalline gold in a solvent is also incredibly useful in the field of microcontact lithography, where the dissolved nanoparticles can be used as a sort of metallic ink which will change back to the bulk gold phase when the protecting thiol groups are forced off during heating.[6]. This method can then be used to create all kinds of useful devices, including a

variety of microelectromechanical systems.[7].

There is no precise definition for the size at which a particle becomes a nanoparticle, but for semiconductors, the energy difference between levels is on the order of $k_B 300°K$ at around 20 nm where for metals this typically occurs below 5 nm. Typically, the term nanoparticle is at least restricted to particles with diameter less than a micron.

1.2.1 Directional Bonding

Defects Available for Reaction

A. Jackson et al. demonstrated that multiple types of thiols on the surface of a gold nanoparticle form spiral or parallel ripple domains instead of disordered phase-separated domains as with a planar gold surface.[1] These rippled nanoparticles should exhibit two polar defects, one at each pole where the SAM is more reactive. This suggests that a reaction in which we place a molecule at each of these poles would allow for the possibility of a bond with 180° directionality. The premise of this project is that these polar defects are of higher energy than all other defects on a nanocrystal.

The primary sources of defects on a nanocrystalline material with multiple types of thiols are (in approximate order of expected magnitude of the effect):

1. Polar defects from phase separation of thiols[1]
2. Non-polar defects from phase separation of thiols
3. Vertices on the gold lattice[8]
4. Twinning boundaries
5. Adhered impurities
6. Random thermal defects in the monolayer

A common way to alter the composition of the SAM on the surface of a gold nanoparticle is through place exchange reactions. It is known that an equilibrium will be reached between surface concentration and concentration in solution.[9] The time scale for this equilibrium is dependant on the reactivity of the SAM, as well as the mean free path for the particles (large particles have more trouble place exchanging) as well as standard effects which could prevent interaction such as steric hindrance. For a standard nanoparticle, we believe the time for complete place exchange to occur is on the order of hours.

Non-polar defects from phase separation of thiols could be caused by the reported alternation of thiol domains on the surface of a multiple-thiol nanoparticle. These defects would likely be quite reactive to place exchange, but would be less reactive than the defects at the polar defects these alternating domains would cause.

Another source of non-polar defects would occur on thiols for which it was not energetically favorable to form the above described alternating structure. In this

case, the thiols would likely phase separate into two domains with an equator. This equator should show reactivity similar to that of the non-polar defects described for the alternating structure. It could be distinguished from a defect caused by the alternating structure because the defect is equatorial instead of isotropic.

A small nanocrystal of gold forms into an octahedron. As with all octahedrons, this means there are eight vertices at which there are more dangling bonds than anywhere else on the surface. These sites are demonstrated to be more reactive than the rest of the surface by Murray et al.[8] These sites should be distinguishable from other defects because there are eight available reaction sites instead of two, an equator, or a uniform distribution.

The remaining sources of defects are going to be of low impact, twinning because it should not occur in the nanoparticles studied, impurities because of the presumably low concentration of impurities in the system, and random thermal defects because of the very high strength of thiol-gold and gold-gold bonds.

Activation Chemistry Using Defect Sites

Due to the hopefully heightened reactivity at the poles of mixed-thiol nanoparticles, a ratio of 2:1 plus a small excess of a replacement alkane thiol to nanoparticle should result in only two replaced groups in the nanoparticle SAM, one at each pole, given that the time of reaction is significantly less than the time constant of the place exchange for the rest of the thiols on the nanoparticle. The poles repel each other to reduce energy, causing them to, on average, point in opposite directions from the nanoparticle center. The combination of these two effects allows the potential for a directional bond on the surface of a nanoparticle.

1.2.2 Selective Bonding

Selective bonding is vital to form complex self-assembled systems. While simple directional bonding does allow for simple systems to form, the introduction of selectivity allows for the creation of much more complex shapes, as is discussed in chapter five.

The selectivity in the systems studied comes from standard chemistry techniques. Initially, amine/acid chemistries are uses to create peptide linkages between the poles of nanoparticles. In a peptide linkage, an amine group and an acid group react to produce a peptide bond and a water molecule. This is selective in that amine enabled particles will not link to other amine particles, only to acid enabled particles.

$$-COOH + H_2N- \rightarrow -CONH - + H_2O \tag{1.1}$$

There is similar chemistry possible between an acid and an alcohol. This forms an ester linkage.

$$-COOH + HO- \rightarrow -COO - + H_2O \tag{1.2}$$

In this work, we avoid the problem of ester linkage interaction by using carbodiimide chemistry to activate the acid groups and prevent interaction with alcohol while using a diamine to link the two activated acid groups together.

In chapters three and five, techniques for using DNA hybridization as a selective linkage are discussed. DNA represents the optimal linkage machinery from an engineering point of view, as two sequences need to be complementary to a very high precision to bind- very small and easily accomplished alterations to DNA sequence can result in very significant changes to the final self-assembled system.

Chapter 2

The use of peptide linkages to form long chains of nanoparticles.

One method by which it is possible to achieve selective, directional bonds with nanoparticles is through polymerization linkage chemistries. Such chemistries include peptides, which are used in these experiments for their stability, esters, ureas, and many others. The general design principle at use here is to create what is essentially a huge copolymer with a nanoparticle as a monomer. (Fig A-1)

2.1 Experimental Requirements

The success of this experiment depends on the ability to demonstrate that linking between nanoparticles has occurred such that there is statistical evidence showing an increase in the number of chains over what would be expected in an unaltered sample.

The primary mechanism by which nanoparticles might bind together is interdigitation.[10] Interdigitation will generally be easily identifiable because it forms large clusters of close-packed nanoparticles with a spacing of roughly the thickness of the SAM. Our chains, on the other hand, should have a slightly larger spacing (the ends of the molecules are binding, so the spacing should be more like twice the thickness of the SAM).

However, with the complexity of the SAMs used on the nanoparticles in this system, we also have to take into account undesired chemical reactions with the non-active part of the layer. As peptides (amine-acid) linkages are being used, the primary worry is other amine or acid groups. While the possibility of ester linkages forming is present, this is mitigated by the use of diamide chemistry.

An adequate proof that there is a reaction going on linking up nanoparticles would be given by statistics showing that if all clusters of nanoparticles are ignored (assuming they are interdigitated), the remaining system has significantly more and longer chains than appear to be present in a random assortment of particles. These micrographs can be produced with TEM, though this makes it difficult to maintain a constant concentration across samples.

2.2 Nanoparticle Synthesis

In order to allow flexibility in the types of structures to be built, nanoparticles will be synthesized in two ways- a standard one-phase reduction reaction and by thiolation of commercially available gold and silver nanoparticles.

The one-phase reduction reaction will result in gold nanoparticles with size on the order of 4 nm. They were synthesized according to the following procedure:

1. 200 mL absolute Et-OH stirred in a 500 mL round bottom flask on an ice bath for 10 minutes. Stirring is never discontinued.
2. 0.9 mmol $HAuCl_4H_2O$ (355 mg) are dissolved and stirred for 10 minutes.
3. 0.9 mmol of thiols are dissolved in a small amount of Et-OH and added and stirred for 10 minutes.
4. 1 g $NaBH_4$ is stirred in 200 mL of absolute Et-OH and filtered into a dropping funnel.
5. Filtered $NaBH_4$ is added drop by drop at about 30 second intervals into gold/thiol mixture either with pipette or carefully with dropping funnel.
6. Solution will become darker until the solution is black and opaque. At this point, addition of $NaBH_4$ can be increased. If the solution turns gold, the synthesis has failed and gold is precipitating from solution in the bulk phase.
7. After $NaBH_4$ is completely added, the solution is stirred for 30 minutes and refrigerated overnight to precipitate nanoparticles.
8. The solution is filtered with quantitative filter paper, washed with Et-OH, H_2O, and acetone.

The choice of thiols for use in this stage of the experiment needs to not contain any alcohol, amine, or acid groups as discussed above. Thus, nonane thiol and mercaptohexanol were used in a 1:2 ratio to produce the rippled nanoparticles. The resulting nanoparticles were soluble in DMF.

To place these same ligands on larger gold and silver nanoparticles, we used colloid purchased commercially and then thiolated the larger particles.

This procedure utilizes:

- 20 nm Gold colloid (GC20) in aqueous solution from BBInternational, as received
- 50 nm Gold colloid (GC50) in aqueous solution from BBInternational, as received
- 20 nm Silver colloid (SC20) in aqueous solution from BBInternational, as received

- 40 nm Silver colloid (SC40) in aqueous solution from BBInternational, as received
- N,N-Dimethylformamide (DMF) 99.8% from Sigma-Aldrich, as received
- *6-Mercapto-1-hexanol (MH) 97% from Aldrich, as received*
- *Nonane thiol (NT) 95% from Aldrich, as received*

The procedure for putting the DMF-soluble ligands on gold and silver colloids is to force the colloid into DMF from the as received water solution and then thiolate.

1. Place $50mL$ of colloid in a round-bottom flask (greater than $150mL$).
2. Add $50mL$ of DMF to flask. This is slightly exothermic.
3. Evaporate off water using Rotovapor at 50°C at $775mmHg$. Completion time is determined by a visual comparison of the volume in the condenser flask to the volume remaining in the solution of nanoparticles.
4. Add thiols in a total ratio of 1:1 with the surface atoms on the colloid. $20nm$ particles should have $\approx$ 46242 surface atoms each. $40nm$ particles should have $\approx$ 74799 surface atoms each. $50nm$ particles should have $\approx$ 190462 surface atoms each.
5. Wrap flask in aluminum foil to protect the DMF from light, and stir overnight to allow full thiolation to occur.

2.3 Nanoparticle Activation and Polymerization

Roughly 5 mg of the nanoparticles were then dissolved in 5 mL of tetrahydrofuran (THF). The next step for polymerizing the nanoparticles into chains is to activate them with amine and acid groups. This was done by taking two equal molarity solutions of the nanoparticles and adding to one sample a 4:1 ratio of 11-Mercaptoundecanoic acid 95% (MUA) from Aldrich, as received) to the nanoparticles.

After 15 minutes of stirring, 15 mL of deionized water was added to the solution to cause precipitation, and the resulting mixture was centrifuged at 3000 RPMs. The liquid was removed and the nanoparticles were dried to stop the place exchange reaction under nitrogen.

The nanoparticles were activated with carbodiamide chemistry. 1 mg of the pole-functionalized particles were dissolved in dichloromethane (DCM). A 500-fold excess of N-hydroxysuccinimide (NHS) and 1-ethyl-3-(3-dimethylaminopropyl)-carbodiimide (EDC) in demethylformamide (DMF) were then added to the nanoparticle solution. The result was then filtered with a Sephadex^{TM} column.

5 mg of nanoparticles were then mixed with a 100-fold excess of 1,7 diaminoheptane to link them together. The solutions were left stirring overnight to equilibrate,

and were subsequently left in solution indefinately with no change in the number or concentration of chains from the samples taken after one night.

2.4 Sample Preparation and Analysis

The samples of polymerized nanoparticles were then deposited onto a carbon TEM grid and micrographs were taken. These micrographs show a visibly obvious increase in the number and length of chains created compared to previous unlinked samples, and also show some interdigitation effects. Chains linked via polymerization chemistries are shown in Fig. A-2 (a,b).

Unfortunately, while the analysis of these chains does offer sufficient proof of linking chemistry creating chains, as well as sufficient proof that this linking is occuring via functionalization of defects on the nanoparticle, there is as of yet insufficient proof that these defects are polar. The minor additional experiments required to demonstrate the directionality of these defects is discussed in chapter five.

Chapter 3

The use of DNA to form long chains of nanoparticles.

An interesting aspect of self-assembly is the ability to create immensely more complicated shapes when selectivity is introduced. For instance, this allows for the ability to create chains of alternating types or sizes of nanoparticles. This ability is easily and conveniently realized through the use of DNA as a binding agent.

3.1 Distinguishing Features of DNA

DNA is a particularly well-suited molecule to the method of defect functionalization described in this paper. The primary reasons for this suitability are:

1. Selectivity
2. Large Size
3. High Stability
4. Few side-reactions

The first reason is the most important, as it allows us to form more complicated shapes as described in Chapter 5. Selectivity is very strong in DNA, as a mismatch of only a few base pairs will result in no binding event for a 16-mer. In addition, it is possible to synthesize DNA with a fairly high accuracy, and with each additional base pair in the chain, the number of possible permuations increases by a factor of four- this gives the potential for algorithmic design of DNA-based self-assembled systems.

Large size is particularly important for the defect functionalization method of self-assembly. The large size of the DNA molecule results in a very low probability of place exchange- it is so much larger than the mercaptohexanol or mercaptoundecanoic acid being used elsewhere on the SAM that the time constant for place exchange on a uniform shell is extremely large. However, at a defect, the DNA is able

to place exchange in less than 15 minutes, giving a ratio of rate constants of over a hundred.

DNA is also very stable once hybridized with it's complementary strand, and there are few side-reactions which could make results more confusing. This will make data easier to analyze, and result in a much cleaner overall system.

3.2 Experimental Procedure

The experimental methods used to create chains with DNA differ only in minor ways from the methods used for peptide linkages. The primary experimental difference was the necessity for the nanoparticles to be soluble in water. To accomplish this, a thiol mixture of mercaptoundecanoic acid and mercaptohexanol was used. The nanoparticles coated with these two ligands was readily soluble in millipore H_2O.

In the pole-functionalization stage of the procedure, two molecules were used, both thiolated DNA sequences.

- $5' - HS - C_6H_{12} - ACGCAACTTCGGGCTCTT - 3'$
- $5' - HS - C_6H_{12} - AAGAGCCCGAAGTTGCGT - 3'$

The nanoparticles were pole functionalized in two batches by dissolving the DNA in 5 mL phosphate buffer solution containing 1 mg of the water soluble nanoparticles at a roughly 4:1 molar ratio of DNA to nanoparticle. After 15 minutes, again the solution was quenched and purified via centrifugation at 3000 RPM.

The complementary pole-functionalized nanoparticles were then redissolved in millipore H_2O with 1M NaCl buffer solution to provide appropriate ionic strength for rapid hybridization.

3.3 Results

Explanation of the statistical analysis of the chains is presented in Chapter 4, an example chain is shown in Fig. A-2 (C). The samples showed a clear increase in the length and number of nanoparticle chains, and qualitiatively appears to be better than the polymer chemistry. Unfortunately, an insufficient number of samples were analyzed to conclusively demonstrate this effect.

As with the peptide linked nanoparticles, the data collected demonstrated clear linking chemistry and defect reactions, but did not yet adequately address the possibility of non-polar defects contributing to the chemistry. This is discussed in chapter five.

Chapter 4

Chain Data Analysis Software

To gather statistical information about the length and number of particles in chains, a matlab program was written. To summarize briefly what it does, it takes as input characteristic values of the system such as the lengths at which two particles are defined to be connected, and an image. It outputs vectors containing the number of clusters and chains of various lengths the program found, as well as an image overlaid with color to provide a visual map of the results.

The code is commented to explain what it is doing at all stages of calculation.

4.1 chaincount.m

```
function [numparticles,chains,clusters,RGB]=
chaincount(filename,reduced_quality_filename,lowerlimit,upperlimit,erode)

% function [numparticles,chains,clusters]=
% chaincount(filename,lowerlimit,upperlimit,erode)
%
% numparticles - number of particles
% chains - chain vector
% clusters - cluster vector
% filename - filename of image                                          10
% lowerlimit - lower limit for center-to-center distance to be
%              considered a chain
% upperlimit - upper limit for center-to-center distance to be
%              considered a chain
% erode - size below which to ignore a particle

% This reads the given image file into a two-dimensional indexed
% matrix named indimg.
[indimg,MAP]=imread(filename);
display(filename);                                                    20
display('successfully read');

% This changes the indexed image indimg to a matrix of brightness
% values (greyscale).
img=ind2gray(indimg,MAP);
```

```
% This stores the original resolution of the image so that if a
% lower resolution output image is requred (for memory problems),
% the image analysis can still be done on the full resolution
% original image and then be properly mapped onto the smaller
% image.
original_resolution=length(indimg);
clear indimg MAP;
display('grayscale finished');

% This sets the threshold for which particles must be darker by
% averaging the minimum and maximum brightness on the image. We
% should watch out for borders on the image. In practice, this is
% done by first using The Gimp 2.2 to make a threshold and this is
% just here for redundancy or a subsequent more advanced version of
% the software.
threshold=(min(min(img))+max(max(img)))/2;
display('thresholding done');

% This gives a matrix of ones at the center of every particle by
% setting every point in the img matrix with brightness less than
% the threshold variable to one and then using imerode to collapse
% each distinct particle of ones into a single one in the
% matrix. Ideally, I would use bwulterode here; unfortunately, this
% function doesn't deal with non-integer centers in the way I would
% like, instead eroding to two or four points if the center is
% between integer values. Thus, I use imerode instead to remove any
% noise in the sample (this will erase any clusters of ones which
% are smaller than the value of erode).

preparticles=imerode(img<threshold,ones(erode));
display('initial erosion complete');
clear threshold img MAP;

% bwlabel is then used to number the particles so that they can be
% distinguished easily later on. Each one in the image is indexed
% and now the cluster or single one where the center of each
% particle is is a number representing the index of that particle.
indexedparticles=bwlabel(preparticles);
clear preparticles;
display('particles indexed');

% This counts the total number of particles for error checking
% later on.
numparticles=max(max(indexedparticles));
display(numparticles);

% This step is one of the most time consuming of the entire
% function, and is necessary because of the drawback in bwulterode
% mentioned above. It goes to each indexed particle, one by one,
% finds the center through averaging the minimum and maximum
% location values in both the x and y directions, and then creates
% a new matrix particles with only a one at the actual center of
% the particle. This takes long enough on a 2.8 GHz machine that I
```

```
% put in a counter to tick off progress as this works through the
% problem.
display('beginning total erosion');
c=1;
for i=1:1:numparticles
  [y,x]=find(indexedparticles==i);
  particles(round((max(y)+min(y))/2),round((max(x)+min(x))/2))=1;
  percentdone=round(i/numparticles*100);
  if percentdone>=10*c
    display(percentdone);
    c=c+1;
  end
end
clear c;

display('erosion complete');

% At this point, the original indices of the particles are
% ignored. Instead, the find function is used to generate a vector
% of the coordinates of each particle. The index of the particle in
% this vector is used henceforth instead of the one assigned by
% bwlabel.
[y,x]=find(particles);
display('particles found');

% This function calculates a distance matrix similar to the type
% you will find in most common maps giving the direct linear
% distance between any two of the particles.
distances=dist([y';x']);
display('distances found');

% This creates a matrix which puts a one everywhere that the
% center-to-center distance is between the thresholds set by the
% user at call time, and a zero otherwise (binary, are these two
% particles connected?) In linear algebra terms, this is called an
% adjacency matrix. The matrix is made sparse to free up memory.
connections=sparse((upperlimit>distances & distances>lowerlimit));
display('connections found');
clear distances;

% This brief loop changes the adjacency matrix manually such that
% particles are not connected to themselves.
w=length(connections);
for i=1:w
  connections(i,i)=0;
end

% This defines two vectors, chains and clusters, which contain the
% number of chains or clusters (respectively) found by the program
% as it walks through the adjacency matrix.
chains(1)=0;
clusters(1)=0;

% This segment of code loads a reduced quality RGB image for
```

```
% output. Loading the full color image into RAM through MATLAB
% produced a number of crashes before the problem was isolated.
display('trying to load reduced quality RGB for output');
[indimg,MAP]=imread(reduced_quality_filename);
RGB=ind2rgb(indimg,MAP);

% This segment of code redefines the scales so that the x and y                    140
% locations of the centers of particles discovered previously is
% now scaled to line up with the lower quality output image.
reduced_resolution=length(indimg);
scaling_factor=reduced_resolution/original_resolution;
display('reduced quality RGB for output loaded');
clear indimg MAP;
x=round(x*scaling_factor);
y=round(y*scaling_factor);

[heig,widt,dep]=size(RGB);                                                       150
i=1;

% This loop finds any lone particles in the adjacency matrix (which
% means that the vector of their connections, connections(1,:) is
% the empty set), colors them in the output image, and removes them
% from the adjacency matrix to save computation later on. It also
% increments the number of one-particle long chains in the chains
% vector. At the end, this number is needed for comparison between
% the number of particles found and the number counted at the
% beginning of the program.                                                       160
while i<=w
  if length(find(connections(i,:)))==0
    connections(i,:)=[];
    connections(:,i)=[];
    chains(1)=chains(1)+1;
    lowerl=max([round(y(i)-lowerlimit*scaling_factor/2),1]);
    upperl=min([round(y(i)+lowerlimit*scaling_factor/2),heig]);
    for l=lowerl:upperl
      lowerj=max([1,round(x(i)-lowerlimit*scaling_factor/2)]);
      upperj=min([widt,round(x(i)+lowerlimit*scaling_factor/2)]);                170
      for j=lowerj:upperj
        RGB(l,j,1)=0;
        RGB(l,j,2)=1;
        RGB(l,j,3)=0;
      end
    end
    x(i)=[];
    y(i)=[];
    i=i-1;
  end                                                                            180
  i=i+1;
  w=length(connections);
end

clear indexedparticles;

display('lone particles removed from connection matrix');
```

```
b=length(connections);
                                                                    190
% This is the meat of the program, which walks down the adjacency
% matrix of particles to identify all the particles which seem to
% be connected linearly. It then checks to see if any particles
% have more than two connections, which indicates the walk doubled
% back. Any walks which double back are defined as clusters while
% walks of entirely unique particles are defined as chains.

for i=1:b
  w=length(connections);
  if w<1                                                            200
    break;
  end

  % This calles the chaincount_helper function which looks at the
  % connections matrix and returns two pieces of information, temp,
  % which is the new connection matrix with the connections between
  % particles in ind replaced with zeros, and ind which is a list
  % of the indices of the  % particles found by the
  % chaincount_helper function.
  [temp,ind]=chaincount_helper(connections);                        210
  len=length(ind);

  % This looks at every particle found in the walk, and sees how
  % many particles it is connected to in the original connections
  % matrix through looking at the length of the find function on
  % the connectivity vector for that particle. If this number is
  % greater than two, the walk must be a cluster (more than two
  % connections to a single particle implies a non-linear walk).
  cluster=0;
  for j=1:len                                                       220
    if length(find(connections(ind(j),:))) >2
      cluster=1;
    end
  end

  % This removes any doubly counted particles in ind and orders
  % them numerically for simplicity.
  orderedindex=union(ind,ind);
  clear ind;
                                                                    230
  % Now that we know all particles in a walk and whether the walk
  % was a cluster or a chain, we increment the appropriate variable
  % in chains or cluster for the length of the walk.
  if cluster==0
    he=length(chains);
    if len>he
      chains(len)=0;
    end
    chains(len)=chains(len)+1;
                                                                    240
    % Colors the dark circle red to represent a chain.
```

```
   for n=1:length(orderedindex)
...
lowerl=max([round(y(orderedindex(n))-lowerlimit*scaling_factor/2),1]);
...
upperl=min([round(y(orderedindex(n))+lowerlimit*scaling_factor/2),heig]);
     for l=lowerl:upperl
...
lowerj=max([1,round(x(orderedindex(n))-lowerlimit*scaling_factor/2)]);
...                                                                          250
upperj=min([widt,round(x(orderedindex(n))+lowerlimit*scaling_factor/2)]);
       for j=lowerj:upperj
         RGB(l,j,1)=1;
         RGB(l,j,2)=0;
         RGB(l,j,3)=0;
       end
     end
   end

   % This following two segments of code then draws a line between            260
   % adjacent particles in the chain to make it visibly clear what
   % the program identified as being connected. These are drawn
   % both by following the x direction and calculating the y
   % location and vice versa to prevent particles with very
   % similar x or y values from only being connected by a single
   % dot or some other appropriately difficult to see line.
   for n=1:(length(orderedindex)-1)
     for m=n+1:length(orderedindex)
       if connections(orderedindex(n),orderedindex(m))==1
         if (x(orderedindex(m))-x(orderedindex(n)))~=0                       270
...
slope=(y(orderedindex(m))-y(orderedindex(n)))/(x(orderedindex(m))-x(orderedindex(n)));
         else
           slope=(y(orderedindex(m))-y(orderedindex(n)));
         end
         for l=1:(x(orderedindex(m))-x(orderedindex(n)))
           ycoord=max([round(y(orderedindex(n))+slope*l),1]);
           ycoord=min([ycoord,heig]);
           xcoord=max([1,round(x(orderedindex(n))+l)]);
           xcoord=min([xcoord,widt]);                                        280
           RGB(ycoord,xcoord,1)=0;
           RGB(ycoord,xcoord,2)=0;
           RGB(ycoord,xcoord,3)=1;
         end
         clear slope;
       end
     end
   end

   for n=1:(length(orderedindex)-1)                                          290
     for m=n+1:length(orderedindex)
       if connections(orderedindex(n),orderedindex(m))==1
         if (y(orderedindex(m))-y(orderedindex(n)))~=0
...
slope=(x(orderedindex(m))-x(orderedindex(n)))/(y(orderedindex(m))-y(orderedindex(n)));
```

```
        else
          slope=(x(orderedindex(m))-x(orderedindex(n)));
        end
        for l=1:(y(orderedindex(m))-y(orderedindex(n)))
          xcoord=max([round(x(orderedindex(n))+slope*l),1]);                    300
          xcoord=min([xcoord,widt]);
          ycoord=max([1,round(y(orderedindex(n))+l)]);
          ycoord=min([ycoord,heig]);
          RGB(ycoord,xcoord,1)=0;
          RGB(ycoord,xcoord,2)=0;
          RGB(ycoord,xcoord,3)=1;
        end
        clear slope;
      end
    end                                                                         310
  end

end

if cluster==1
  he=length(clusters);
  if len>he
    clusters(len)=0;
  end
  clusters(len)=clusters(len)+1;                                                320
  %   display('cluster found');

  for n=1:length(orderedindex)
...
lowerl=max([round(y(orderedindex(n))-lowerlimit*scaling_factor/2),1]);
...
upperl=min([round(y(orderedindex(n))+lowerlimit*scaling_factor/2),heig]);
    for l=lowerl:upperl
...
lowerj=max([1,round(x(orderedindex(n))-lowerlimit*scaling_factor/2)]);          330
...
upperj=min([widt,round(x(orderedindex(n))+lowerlimit*scaling_factor/2)]);
      for j=lowerj:upperj
          RGB(l,j,1)=0;
          RGB(l,j,2)=0;
          RGB(l,j,3)=1;
      end
    end
  end
end                                                                             340

% Now that the connections have been adequately followed, the
% original connections matrix is replaced by the temp matrix
% generated by chaincount_helper which removed the particles
% found by the walk from the adjacency matrix. This results in
% increasing speed of calculation as the adjacency matrix rapidly
% shrinks to nothing.
connections=temp;
```

```
  % This segment of code actually carries out the shrinking of the
  % adjacency matrix by removing the rows and columns of zeros
  % generated when chaincount_helper deleted the connections
  % between the particles already found.
  m=1;
  while m<=w
    wid=length(connections);

    if m>wid
      break;
    end

    if sum(connections(m,:))+sum(connections(:,m))==0
      connections(m,:)=[];
      connections(:,m)=[];
      x(m)=[];
      y(m)=[];
      m=m-1;
    end
    m=m+1;
  end
end
```

```
function [cor,ind]=chaincount_helper(cor)
% This helper function takes a correlation matrix generated in
% chaincount and outputs a vector ind of the particles involved in
% a walk down the adjacency matrix beginning at the first indexed
% particle along with a new adjacency matrix where the connections
% between those particles have been removed.

l=length(cor);
c=0;
ind=1;
while c<length(ind)
  i=ind(c+1);
  i_tmp=find(cor(i,:));
  ind=[ind,setdiff(i_tmp,ind)];
  cor(i,:)=zeros(1,l);
  cor(:,i)=zeros(l,1);
  c=c+1;
  if length(find(cor(ind(c+1:length(ind)),:)))==0
    break;
  end
end
```

4.2 Conclusions

The data collected from more than 40 samples with a total particle population exceeding 50,000 showed an average yield[1] of 20% (standard deviation of 8%) of chains compared with 3-5% found in control experiments without polar linking chemistry. As might be expected, there was an exponential decay in the number of particles in chains of increasing length. A typical result of an image analysis is showin in Fig. A-3. A typical graph of the number of particles in a chain of a given length is shown in Fig. A-4.

The consistent result across samples was unexpected, as differing times and linking chemistries were assumed to be the rate determining step. Instead, this consistency suggests that the step determining the equilibrium chain length was the gold-thiol equilibrium constant.

Unfortunately, due to the relatively high fraction of particles in clusters, it is difficult to demonstrate that the chains found were the result of polar defects, or simple stoichiometric or statistical probability. For example, if the vertices of the gold cluster were more reactive than any polar defect, but the 4:1 ratio of DNA:Au limited the number of defects per nanoparticle which were functionalized, you would still see linear chains. Solutions for isolating this effect are discussed in chapter five.

[1]Where average yield is defined as the number of particles in chains divided by the total number of particles.

Chapter 5

Analysis of Chains

5.1 What was Demonstrated by this Thesis.

As mentioned in previous chapters, the statistical analysis of TEM micrographs clearly demonstrated that

1. Linking chemistry was causing a statistically significant number of chains to form compared to a system with no linking chemistry.

2. Defect chemistry was occuring.

The first of these two claims is demonstrated by the factor of about five difference in the number of particles in chains under samples which underwent linking chemistry versus a control sample. As discussed, 20% (standard deviation of 8%) of chains were found in the samples which underwent functionalization and linking, compared with 3-5% found in control samples.

The second claim is shown in the time of reaction required to functionalize the nanoparticles. Previous experiments have demonstrated that the time constants for place exchange on a nanoparticle are on the order of days[9], even with a twenty-fold excess of solution thiol to cluster bound thiol. This time constant increased as the size of either the solution thiol or the cluster bound thiol increased. In addition, the time constant increases with decreased concentration of thiol in solution.

Previous experiments for relatively small thiol molecules show a reaction time constant of on the order of three days. In our experiment, we used a much larger molecule, both on the cluster and in solution, and had a much lower concentration of solution thiol. These two pieces of information guarantee that any normal place exchange reactions should have taken place on the order of at least three days, if not weeks or months.

In our experiments, DNA functionalized the clusters in under 15 minutes with a roughly 20:1 deficiency of thiol in solution compared to cluster bound thiol[1]. This

[1]We expect 252 surface atoms, and with a 3:1 coordination between surface gold atoms and thiols, there should be 84 thiols per cluster. A 4:1 ratio of DNA in solution to nanoclusters then has a 21:1 cluster bound:solution thiol ratio.

suggests a ratio of reactivities on the order of 10^3, clearly demonstrating the action of defect chemistry.

5.2 Ambiguities in Results for Chain Linking

The concentration of thiol in solution was so small, so if there were many defects, or non-polar defects, stoichiometric considerations could cause linear chains to form despite the nanoparticles being capable of forming linkages in many more directions given enough functionalization molecules.

There are two tests which should answer this question. The more difficult of the two is to change the analysis software to detect bond angles. As the software is currently implemented, it is impossible to include bond angle considerations into the counting algorithm, and this would represent a significant improvement to the software. By detecting non-linear bonds in chains, a statistical measure of the number of potential non-polar defects could be calculated.

The second test is simpler. Add a large excess of DNA to a solution containing both mixed ligand and single ligand nanoparticles ($> 100 : 1$). Because of the large size of DNA, the place exchange reaction should still be slow on non-defect sites. However, given 15 minutes to place exchange, the defect sites on the nanocrystal should be saturated with the functional group.

If our theory is correct, the two polar defects are so much more reactive than the other defect sites that they will still be the only ones functionalized, resulting in roughly identical data to that collected previously. The single ligand nanoparticles will have no defects of high enough reactivity to place exchange, and the number of chains will be comparable to the controls.

If, on the other hand, there are non-polar defects caused by the mixed ligand shell, these nanocrystals should immediately form large clusters instead of linear chains, resulting in an obvious reduction in the number and length of chains observed by the analysis software relative to the numbers of clusters. However, as in the first case the single ligand nanoparticles will not place exchange at all, and will have a chain:cluster ratio similar to that of the controls.

If there are non-polar defects caused by intrinsic properties of the nanocrystal (the eight reactive vertices) dominating the functionalization, then both the single and mixed ligand particles will tend to immediately cluster, lowering the chain:cluster ratio below that of the control.

5.3 Conclusions about Chain Linking Chemistry

In conclusion, the chain linking chemistry seems to have clearly demonstrated the existance of defects and has statistically made a proof of concept that linking chemistries can form chains of nanoparticles. By doing one further simple experiment with a large excess of DNA molecules compared to nanoparticles, it can be determined with a reasonable assurance that the defects are indeed polar in nature.

Chapter 6

Promising Results and Future Directions

6.1 Triangle Groupings of Nanoparticles

To date, we have attempted to self-assemble triangles of nanoparticles. The essential method for forming these triangles is based on work done by N.C. Seeman et al. who used partially matching sequences of DNA to create conjugated DNA with three ends.[11] By first attaching the free ends of these DNA fragments to a gold nanoparticle, it should be possible to self assemble these nanoparticles into a triangle supported by a DNA scaffold. (Fig. A-5)

6.1.1 Selection of appropriate DNA sequences.

The method used by NC Seeman et al.[11] to determine an appropriate sequence of DNA is to use the following criteria:

1. All sequences of quatramers are unique.
2. Each tetramer spanning a branch point does not have it's linear complement present.

In addition, the length of the DNA sequence between the DNA junction and the nanoparticle should be irrelevant due to the rotational symmetry of the DNA molecule; however, due to steric hindrance between adjacent gold nanoparticles, the length of each DNA molecule must be such that

$$L \approx 0.155d \tag{6.1}$$

where L is the length of the DNA molecule and d is the diameter of the gold nanoparticle. This formula is derived from geometrical constraints on close packed spheres.

In addition, the length of the DNA molecule must be sufficient as to prevent denaturization- a length greater than a 10-mer is sufficient to guarantee this.

NC Seeman et al. have already published several sequences capable of forming triangles.[11] These sequences are 16-mers, which are long enough to satisfy both constraints given above. As these sequences are already known to successfully form triangles, we used them here in a thiolated form to allow attachment to gold nanoparticles.

The sequences used are:

- 5′-HS-C_6H_{12}-CAG GCT GTG AGC GGT G-3′
- 5′-HS-C_6H_{12}-GAG GAC CAA CAG CCT G-3′
- 5′-HS-C_6H_{12}-CAC CGC TCT GGT CCT C-3′

The addition of the C_6H_{12} into the chain ensures that the DNA sequence begins beyond the height of the SAM on the surface of the nanoparticle.

6.1.2 Experimental Technique

The experimental techniques used to produce triangular nanoparticle shapes was identical to those used for chains of DNA with three activated nanoparticles being added together for any one experiment. The experiment was carried out for all permutations of a small, medium, and large nanoparticle (three small, two small with one medium, etc.), and some promising results were obtained. A micrograph of one such cluster with a small, medium, and large nanoparticle is shown in Fig. A-10 (b).

Unfortunately, this result was not repeatable enough to be conclusive as of yet and further isolation of the critical processing variables is necessary. It was discovered that time played a critical role, as solutions of three activated nanoparticles left to conjugate for more than 30 minutes failed to form any predictible shapes.

Another very interesting and unexpected system which seems to have been created are very large triangles which seems to be self-assembling system of nanoparticles. This system was created by linking using the above described triangle chemistry with relatively uniform nanoparticles. As can be seen, this system shows a high anisotropy and while it has not yet been demonstrated conclusively that the polar chemistry is forming these systems, it seems very likely and is a worthwhile direction for future research. (Fig. A-6) Interestingly, the triangles seem to exhibit a "hole" in the middle which has yet to be explained. (Fig. A-7)

These triangles were reproducible, but further attempts have failed to reproduce triangles in as large of a yield, with as large a size, or with as much fidelity as the original experiment.(Fig. A-8, A-9) Visual inspection of the more recently attempted super-crystals of nanoparticles shows a very large polydispersity in the nanoparticles. Unfortunately, the individual nanoparticles in Fig. A-6 are not visible, so a comparison cannot be made, but it is reasonable to suspect that if new, more monodisperse nanoparticles were used, they would have a greater tendancy to order.

6.2 Other Interesting Results

Several other interesting shapes were produced, including alternating chains of small/large particles and rings. The small/large alternating chains were made by activating large gold particles with an acid group (MUA) and smaller silver particles with an amine group. These were then mixed together and allowed to polymerize, resulting in a sort of block copolymer of nanoparticles. (Fig. A-10 (a))

The rings were produced by functionalizing gold nanoparticles with MUA and allowing it to form a complex with Ni^{2+}. This is shown under AFM in Fig. A-10 (c). Fig. A-10 (d) shows that this technique of activation chemistry can be applied to other systems, in this case creating a chain of gold nanorods.

6.3 Conclusions and Future Work

This new selective, and hopefully directional linking method has produced chains, triangles, and rings of nanoparticles. In addition, the activation and linking of nanorods demonstrated that this technique is applicable to other nanoscale materials as well.

Questions left unanswered include why large self-assembled triangles are forming, as well as a full description of the mechanics behind triangle formation. In addition, tests on coupling between nanoparticles linked in a chain through either photonic or magnetic measurements could prove to be very interesting. Finally, tests of the electrical properties of these nanoparticles when attached across two leads using the pole chemistry could lead to a new way to synthesize single electron transistors with greater flexibility.

Appendix A

Figures

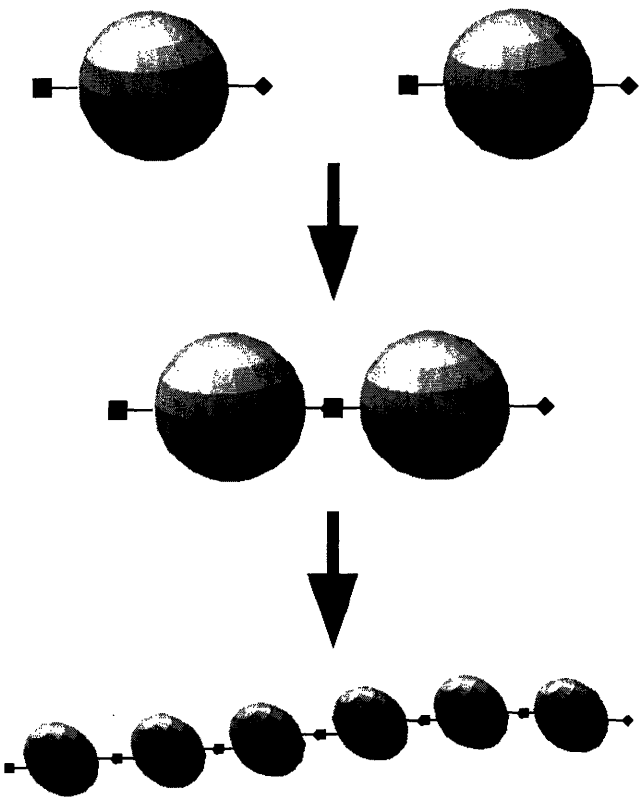

Figure A-1: Cartoon of the polymerization of nanoparticle monomers into a chain.

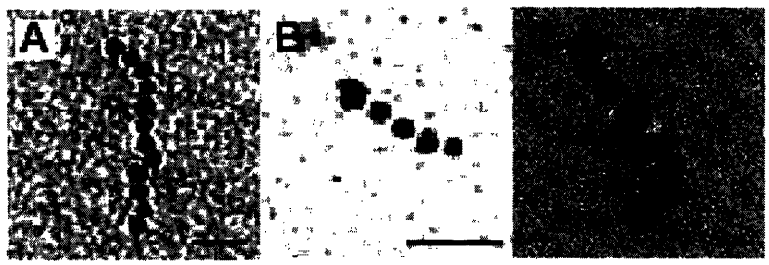

Figure A-2: TEM images of chains of gold nanoparticles. (A) Nanoparticles activated with MUA and 1,7-diaminoheptane (B) 16-aminohexadecane-1-thiol pole functionalized nanoparticles with 1,6,-diisocyanatohexanol (C) Nanoparticles activated half with a single strand of DNA and half with the complementary strand of DNA. Scale bars- 20 nm.

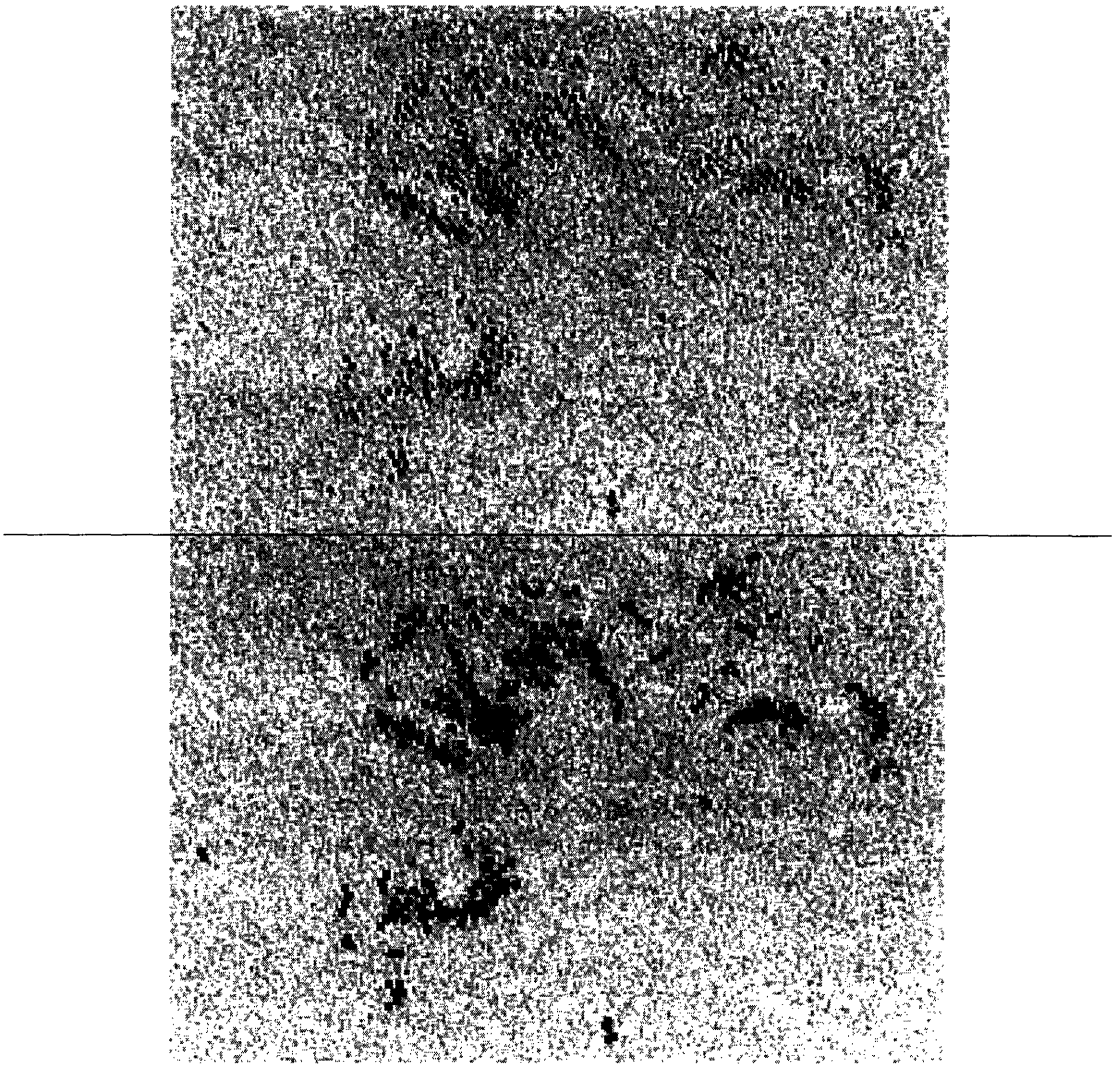

Figure A-3: A typical TEM micrograph before and after image analysis via the Chaincount program. The blue dots represent clusters, the green dots represent single particles, and the red dots represent chains with blue lines indicating found connections between particles.

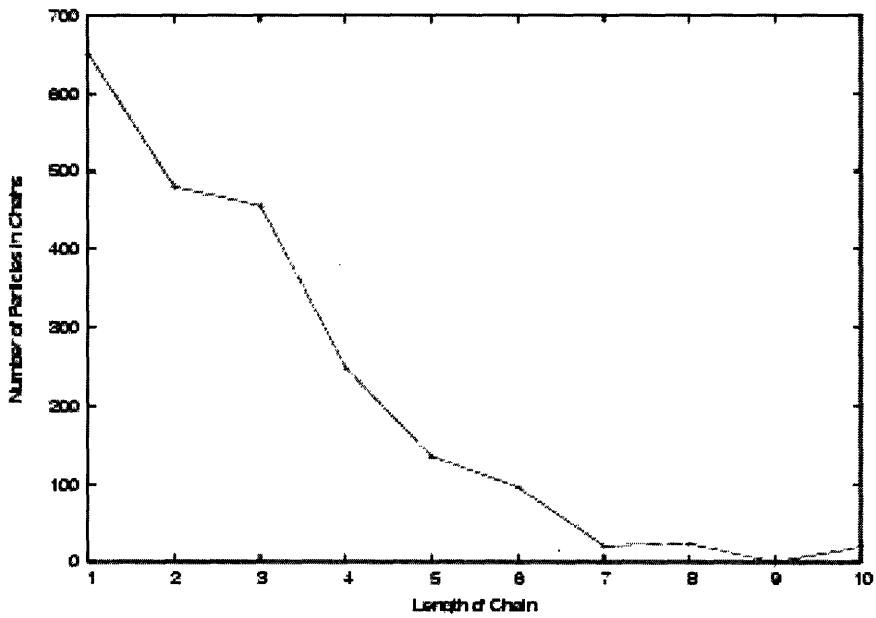

Figure A-4: The number of particles contained in chains of varying lengths for a typical sample analyzed with Chaincount. This shows a roughly exponential decay.

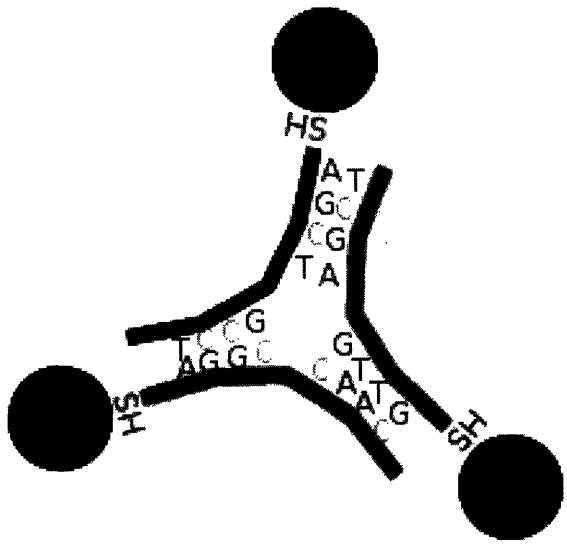

Figure A-5: Cartoon of triangle formation. By matching half of each thiolated DNA strand to half of each of the other two DNA strands in an appropriate sequence, a triangle is formed.

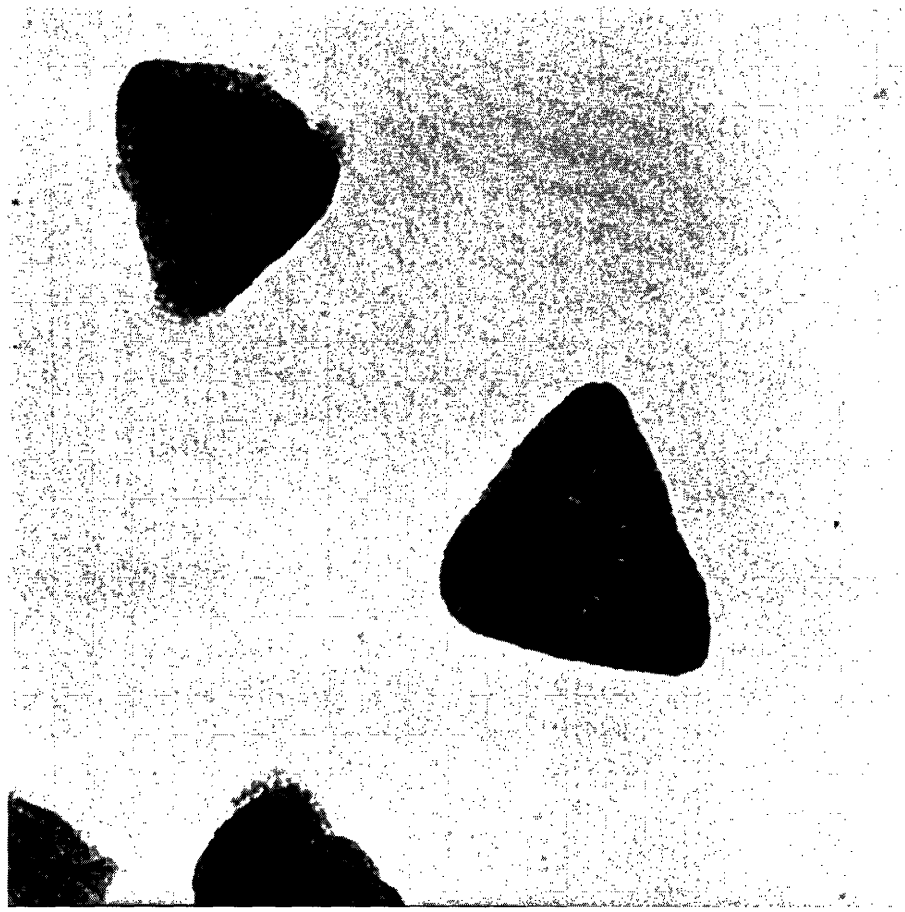

Figure A-6: TEM micrographs which suggest nanoparticles activated to form triangles are self-assembling into vast triangular arrays. No scale bar is available due to TEM malfunction, but they are on the order of a micron across and would be composed of 5 nm particles.

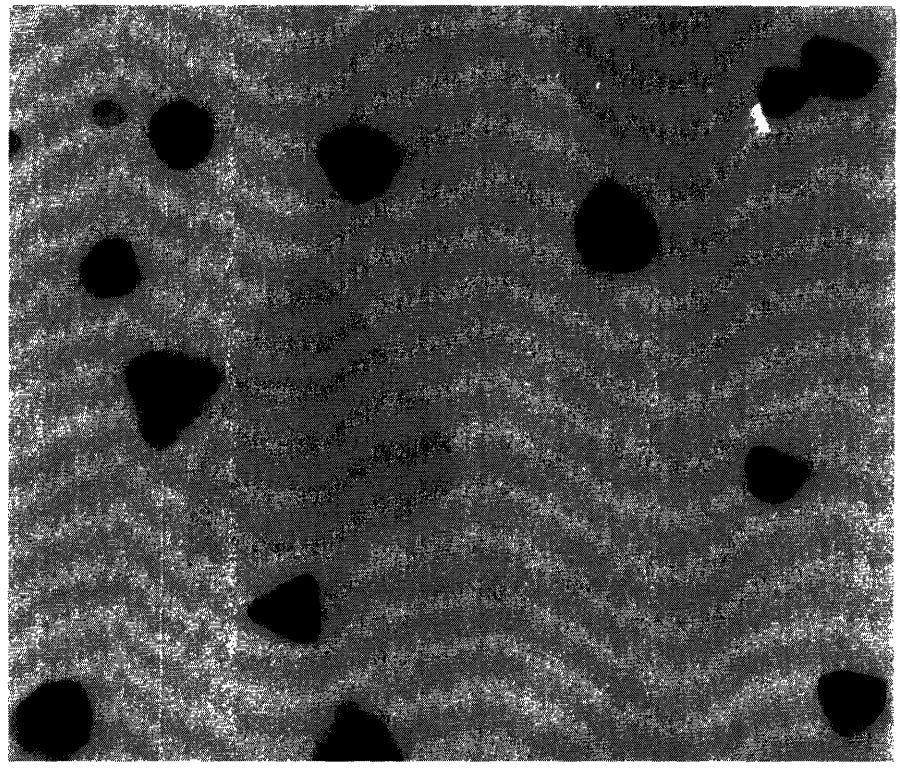

Figure A-7: TEM micrograph of many super-crystalline triangles. These triangles all show a lighter (less dense) spot inside the larger triangle.

Figure A-8: TEM micrograph of more recently formed super-crystals of nanoparticles. This shows less fidelity, and the high polydispersity of the nanoparticles is apparant under inspection of high resolution images.

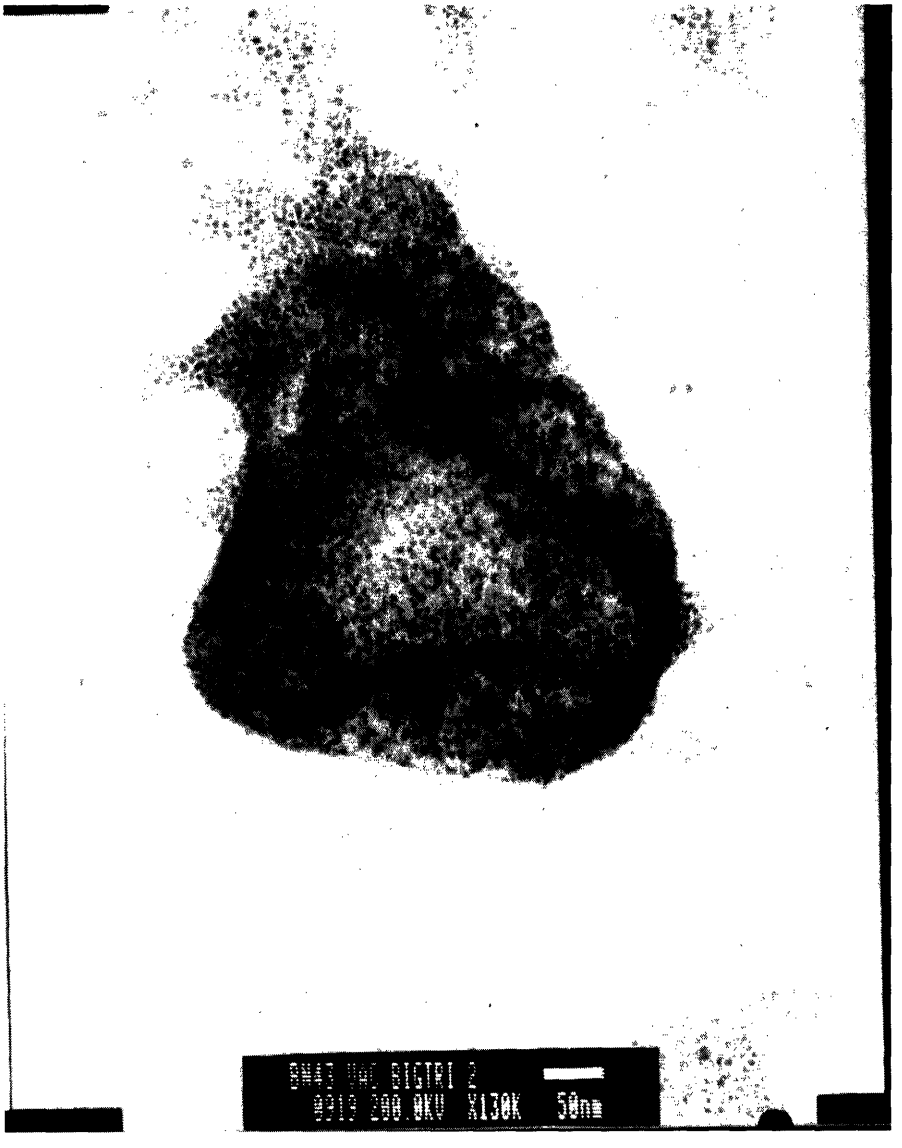

Figure A-9: TEM micrograph of more recently formed super-crystals of nanoparticles. This shows better fidelity than the previous figure, although the polydispersity is even more obvious.

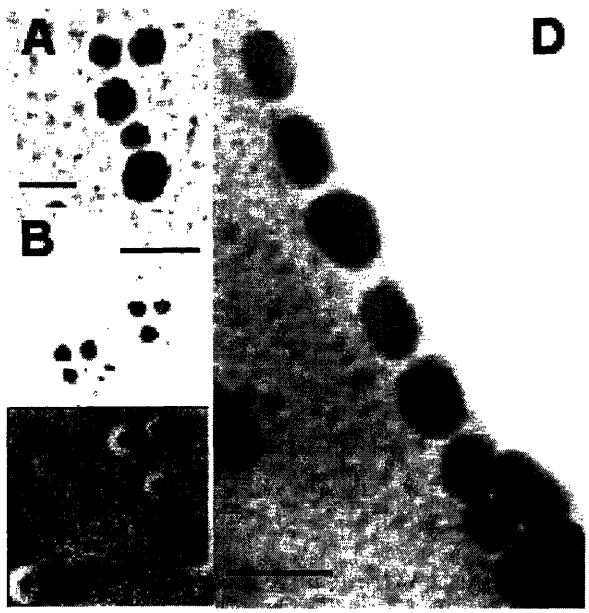

Figure A-10: Micrographs of assemblies of nanomaterials. (A) TEM micrograph of a chain of alternating 50 nm gold particles activated with MUA and 20 nm silver particles activated with amine groups. (B) TEM micrograph of triangles of gold nanoparticles obtained by mixing three solutions containing nanoparticles pole functionalized with 1 of 3 different single stranded DNA molecules designed for form a triangular scaffold. (C) AFM image of rings of MUA functionalized gold nanoparticles linked using Ni^{2+} ions. Scale bar- 200 nm. (D) TEM micrograph of a chain of gold nanorods. The poles were functionalized with MUA and linked with 1, 7-diaminoheptane. (A, B, and D) - Scale bars, 20 nm.

Bibliography

[1] Jackson AM, Myerson JW, and Stellacci F. Spontaneous assembly of subnanometre-ordered domains in the ligand shell of monolayer-protected nanoparticles. *Nature Materials*, 3(5):330–336, May 2004.

[2] Thelander C, Magnusson MH, Deppert K, et al. Gold nanoparticle single-electron transistor with carbon nanotube leads. *Applied Physics Letters*, 79(13):2106–2108, September 2001.

[3] Haes AJ and Van Duyne RP. A unified view of propagating and localized surface plasmon resonance biosensors. *Analytical and Bioanalytical Chemistry*, 379(7-8):920–930, August 2004.

[4] Schmid G, Pfeil R, Boese R, Bandermann F, Meyer S, Calis GHM, and van der Velden JWA. $[Au_{55}\{P(C_6H_5)_3\}_{12}Cl_6]$ - A gold cluster of unusual size. *Chem. Ber.*, 114:3634–3642, 1981.

[5] Hu JH, Johnston KP, and Williams RO. Nanoparticle engineering processes for enhancing the dissolution rates of poorly water soluble drugs. *Drug Development and Industrial Pharmacy*, 30(3):233–245, 2004.

[6] Wilhelm EJ and Jacobson JM. Direct printing of nanoparticles and spin-on-glasses by offset liquid embossing. *Applied Physics Letters*, 84(18):3507–3509, May 2004.

[7] Wilhelm EJ, Neltner BT, and Jacobson JM. Nanoparticle-based micro-electromechanical systems fabricated on plastic. *Applied Physics Letters*, 85(26):6424–6426, December 2004.

[8] Guo R, Song Y, Wang G, and Murray RW. Does core size matter in the kinetics of ligand exchanges of monolayer-protected au clusters? *J. Am. Chem. Soc.*, 127:2752–2757, February 2005.

[9] Hostetler MJ, Templeton AC, and Murray RW. Dynamics of place-exchange reactions on monolayer-protected gold cluster molecules. *Langmuir*, 15(11):3782–3789, May 1999.

[10] Badia A, Singh S, Demers L, Cuccia L, Brown GR, and Lennox RB. Self-assembled monolayers on gold nanoparticles. *Chemistry-A European Journal*, 2(3):359–363, March 1996.

[11] Nadrian C. Seeman. At the crossroads of chemistry, biology, and materials: Structural dna nanotechnology. *Chemistry & Biology*, 10(12):1151–1159, December 2003.